Effect of surface area on the rate of photocatalytic water oxidation as promoted by different manganese oxides

CrossMark

Carminna Ottone [a,b], Marco Armandi [b], Simelys Hernández [a,b], Samir Bensaid [b,*], Marco Fontana [a,b], Candido Fabrizio Pirri [a,b], Guido Saracco [b], Edoardo Garrone [b], Barbara Bonelli [b]

[a] Center for Space Human Robotics, IIT@POLITO, Istituto Italiano di Tecnologia, C.so Trento 21, 10129 Turin, Italy
[b] Applied Science and Technology Department, Politecnico di Torino, C.so Duca degli Abruzzi 24, 10129 Turin, Italy

HIGHLIGHTS

- Mn_2O_3, Mn_3O_4 and MnO_2 were used as catalysts for photocatalytic water oxidation.
- The rate of O_2 production was retrieved from raw data through a mathematical model.
- The activity per unit mass of commercial samples was $Mn_2O_3 > MnO_2 > Mn_3O_4$.
- Only with Mn_3O_4 an increase in SSA obtained by ball milling led to higher reaction rates.

GRAPHICAL ABSTRACT
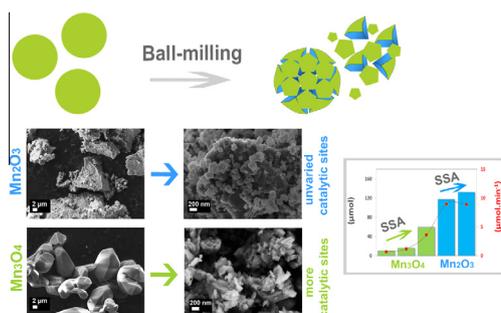
ARTICLE INFO

ABSTRACT

Commercial Mn_2O_3, Mn_3O_4 and MnO_2 and the same after thermal or ball-milling treatments have been examined as catalysts for the photocatalytic water oxidation reaction, using $[Ru(bpy)_3]^{2+}$ as photosensitizer and $S_2O_8^{2-}$ as sacrificial electron acceptor. Tests were performed in a bubbling reactor, allowing the calculation of the actual rate of O_2 evolution as a function of time from raw data (oxygen flow, concentration of dissolved oxygen, DO) through a model able to take into account mass transfer phenomena Hernández et al. [19]. A few parameters are proposed for measuring activity, and comparison among them is made. The activity per unit mass of commercial samples is $Mn_2O_3 > MnO_2 > Mn_3O_4$, in agreement with the literature. Increase in the surface area brought about by milling correspond, as expected, to a steady increase in activity in the case of Mn_3O_4, whereas had no effect with Mn_2O_3. The markedly higher specific surface of Mn_2O_3 and Mn_3O_4 samples obtained by thermal treatment of MnO_2 and a home-made sample, respectively, correspond surprisingly to activities lower than low surface area ball milled samples. Reasons for this are proposed to be a different nature of the surfaces arrived at, because of the different preparation route. A similar study of the effect of surface area for MnO_2 specimens is prevented by their largely amorphous nature. Comparison of present data with those already reported gives further support to the bounty of the model taking into account mass transfer.

© 2015 Elsevier B.V. All rights reserved.

1. Introduction

Dioxygen evolution from water (*i.e.* water oxidation, WO) is a critical step for processes such as water splitting or artificial photosynthesis [1,2]. Thus, much work is being devoted to the development of suitable water oxidation catalysts (WOCs), among which different transition metal oxides (IrO_2, Co_3O_4, RuO_2, Rh_2O_3 and Mn oxides) have been traditionally studied [3–5].

Mn oxides show good activities [6–13], are abundant and low cost. They occur, though, in a wide number of structures and

oxidation states, so constituting a wide field. Recently, Robinson et al. [10] compared different oxide structures (Mn_2O_3, Mn_3O_4, and five structural polymorphs of MnO_2) and found Mn_2O_3 to be the most active. High turnover frequencies and remarkable stability have been also reported for α-MnO_2 and β-MnO_2 nanowires and nanotubes in un-buffered media [7]. Confinement of Mn oxide nanoparticles within a meso-porous silica also resulted in a very active WOC [14]. Actually, many amorphous structures, such as mixed valence (Mn^{4+}/Mn^{3+}) oxides [8] were found to be highly active as compared to crystalline counterparts, under both chemical and photochemical conditions. A disordered Mn oxide layer, electrochemically deposited, also allowed WO at neutral pH with high rates at low overpotentials [15]. It is however difficult to compare results from different laboratories, because of the large number of possible structures, Mn oxidation states, morphologies, and finally measurement techniques.

Recently, we have investigated the activity of WOCs, including Co-APO-5 zeotype [16–18], Co_3O_4 [19], and $BiVO_4$ photocatalyst [20,21]. In the present paper the study is extended to the already beaten track of Mn oxides, focussing attention on two aspects of WO reaction, i.e. the role of the catalytic surface and the reliability of measurements. The former seems to have received little attention so far: the first part of the work was thus devoted to preparing samples with different specific surface area (SSA), both by thermal treatments of known phases and their ball-milling treatment.

As to WOC activity assessment, both electrochemical [15,17,22,23] and sacrificial oxidant [6–12,16,19] methods can be used. Our choice is the latter, as a relatively large amount of oxygen is yielded, thus easing in principle the measurements of turnover numbers (TON) and frequencies (TOF). The sacrificial oxidant was the widely used $Ru(bpy)_3^{2+}/S_2O_8^{2-}$ photosystem [24]. The well documented mechanism of reaction [4] is summarised in Scheme 1 and briefly described in the ESI. Note that without a WO catalyst, no O_2 is produced and $Ru(bpy)_3^{3+}$ decomposes due to OH^- (or water molecules) attack on the bipyridile ring (Eq. (4)) [4,16]. Such a reaction always competes with WO and heavily interferes with it.

A direct comparison of TON and TOF to literature data for photochemical WO with $Ru(bpy)_3^{2+}$ catalyzed by Mn oxides is rather difficult. Besides the sources of variability already listed, several reaction parameters, such as reactants concentrations, catalyst amount, type of buffer, and surface areas affect WO results.

Another degree of freedom in literature reports is the method used for measuring the evolved oxygen. Closed batch reactors are generally used, where O_2 evolution is followed by measuring either the amount of O_2 dissolved (DO) in liquid by a Clark-type electrode [7,9,10] or O_2 partial pressure in the gas headspace by Gas Chromatography (GC), assuming equilibrium between the gas and liquid phases [4,6,8]. The former method generally underestimates the total amount of evolved O_2, mostly because a part of the dissolved gas passes into reactor headspace [8]. On the other hand, classic GC is not suitable for determination of initial rates of production, requiring extraction of gas sample from the reactor headspace for injection.

In our work, the activity of different WOCs was investigated by using a bubbling reactor, in which produced O_2 is removed from the liquid phase by means of a sweeping gas, so to minimize mass transfer limitations to the catalytic reaction. Combined use of Clark electrode and micro Gas Chromatography (μ-GC) allowed us to measure both outlet O_2 flow rate and DO. From these data, a model taking into account mass transfer phenomena [19] gives access to the actual rate of oxygen production as a function of time. In the present paper, both batch and bubbling experiments are reported, the latter to a larger extent.
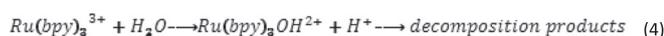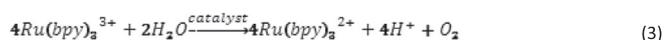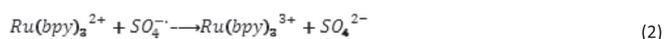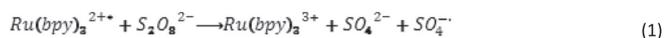
2. Experimental

2.1. Materials

All chemicals ($Ru(bpy)_3Cl_2·6H_2O$ (99.95%), Na_2SO_4, $Na_2S_2O_8$, $Na_2HPO_4·2H_2O$, $NaH_2PO_4·H_2O$) and commercial manganese oxides (hereafter Mn_2O_3-C, MnO_2-C and Mn_3O_4-C) were Sigma–Aldrich. To increase their specific surface area (SSA), Mn_2O_3-C and Mn_3O_4-C powders (initial SSA 2.0 and 0.6 m^2/g, respectively) were mechanically ground in a planetary micro mill (Pulverisette 7, Fritsch), working with 10 balls of stainless steel (10 mm in diameter) at 800 rpm for either 2 or 20 h. Obtained samples are denoted as Mn_xO_y-BMn, were n is the ball milling time in hours. On the other hand, activated porous MnO_2 (Fluka P.N. 63548) was calcined in air at 500 °C for 5 h, with a heating rate of 1 °C min^{-1}, yielding an α-Mn_2O_3 crystalline phase (Mn_2O_3-TT).

A specimen of laboratory-made (LM) Mn oxide was prepared by hydrothermal route, in the attempt to have it in ordered mesoporous form, using a literature recipe for Co_3O_4 [25]. The result was disappointing, but calcination at 500 °C yielded a high SSA specimen of Mn_3O_4 (Mn_3O_4-LM).

2.2. Characterization

Powder X-ray diffraction (XRD) patterns were collected on an X'Pert Phillips diffractometer using Cu Kα radiation = 1.541874 Å (10–80 2θ range; step width = 0.02 2θ; time per step = 2 s) and indexed according to the Powder Data File database (PDF 2000, International Centre of Diffraction Data, Pennsylvania). Average crystallite size was determined through the Debye–Scherrer formula, $D = 0.9\lambda/b \cos\theta$, where λ is the wavelength, b is the full width at half maximum (in radians), 0.9 is the shape factor for spherical particles and θ is the diffraction angle.

Brunauer–Emmett–Teller (BET) Specific Surface Area (SSA) was measured by N_2 adsorption/desorption at 77 K (Quantachrome Autosorb 1C) on samples outgassed at 150 °C for 4 h. When appropriate, BJH (Barrett–Joyner–Halenda) method was applied on desorption branches to calculate pore size distribution (PSD, reported in Fig. S1).

Field Emission Scanning Electron Microscopy (FE-SEM) pictures were collected on a high-resolution instrument (LEO 1525).

Elemental analysis of post-reaction samples were performed by means of X-ray Fluorescence (XRF) on a Rigaku XRF ZSX 100E (3 kW X-ray tube).

2.3. Photocatalytic tests

Two methods have been adopted for measuring the catalytic activity. In one set of experiments, close batch reactors were used in the absence of any stripping gas, so to measure the concentration of DO, hereafter denoted as C_{O_2}, by means of a Clark electrode. A small reactor (20 ml) was used to minimize headspace volume. Reactant concentrations and WOCs amount (mg/L) were the same of bubbling experiments below. Also in this case, any O_2 present was previously removed by flowing Ar through the liquid phase, under dark conditions before measurements. After sealing reactor,

$$Ru(bpy)_3^{2+\ast} + S_2O_8^{2-} \longrightarrow Ru(bpy)_3^{3+} + SO_4^{2-} + SO_4^{-\cdot} \quad (1)$$

$$Ru(bpy)_3^{2+} + SO_4^{-\cdot} \longrightarrow Ru(bpy)_3^{3+} + SO_4^{2-} \quad (2)$$

$$4Ru(bpy)_3^{3+} + 2H_2O \xrightarrow{catalyst} 4Ru(bpy)_3^{2+} + 4H^+ + O_2 \quad (3)$$

$$Ru(bpy)_3^{3+} + H_2O \longrightarrow Ru(bpy)_3OH^{2+} + H^+ \longrightarrow decomposition\ products \quad (4)$$

Scheme 1.